

Yukawa Unification and Unstable Minima of the Supersymmetric Scalar Potential

Amitava Datta ^{*†}

Department of Physics, Visva-Bharati, Santiniketan - 731 235, India

Anirban Kundu [‡] and *Abhijit Samanta* [§]

Department of Physics, Jadavpur University, Calcutta - 700 032, India

February 1, 2008

hep-ph/0007148

Abstract

Motivated by the possibilities of $b - \tau$ or $t - b - \tau$ Yukawa unification in the supersymmetric Grand Unified Theories, we consider the dangerous directions of the supersymmetric potential for large values of $\tan\beta$ ($\gtrsim 30$), in two versions of the minimal supergravity model with and without common soft breaking scalar masses at the GUT scale, where the potential may become unbounded from below. We find that for the common trilinear coupling $A_0 \lesssim 0$ the requirement of $b - \tau$ unification in conjunction with the stability condition on the potential yields highly restrictive sparticle spectra with upper, and in many cases, lower bounds stronger than the available experimental lower bounds, on the soft SUSY breaking common scalar mass and the common gaugino mass. Over a significant region of the parameter space, the model becomes even more restrictive if the common sfermion soft mass is different from the soft mass for the Higgs sector. We also find that the bulk of this restricted parameter space can be probed at the LHC. In models with $t - b - \tau$ Yukawa unification, $A_0 \leq 0$ is ruled out from potential constraints.

PACS no: 12.60.Jv, 14.80.Ly, 14.80.Cp

^{*}Electronic address: adata@juphys.ernet.in

[†]On leave of absence from Jadavpur University.

[‡]Electronic address: akundu@juphys.ernet.in

[§]Electronic address: abhijit@juphys.ernet.in

1 Introduction

If we have to go beyond the Standard Model (SM), for which there are ample motivations, the most popular choice seems to be supersymmetry (SUSY) [1]. With a plethora of new degrees of freedom, it is necessary to constrain them, in addition to direct searches at the colliders, in as many ways as possible so that the parameter space for the SUSY particles may be narrowed down. One of the most useful ways to put such constraints is to consider the dangerous directions of the scalar potential where the potential may be unbounded from below (UFB) or develops a charge and/or color breaking (CCB) minima [2]. This may happen since one now has charged and colored scalar fields in the spectrum, and the possible existence of such a direction would make the standard vacuum unstable. Different directions are chosen by giving vacuum expectation value (VEV) to one or more scalar fields, while keeping the VEVs of the other scalars to zero.

Such constraints, in fact, are very powerful. This may be realized from the fact that the allowed parameter space (APS) for SUSY models is practically unrestricted as one goes for larger and larger values of the soft SUSY breaking parameters (*e.g.*, the universal scalar and gaugino masses, the trilinear coupling, etc.)¹ beyond the kinematic limit of the current high energy colliders. On the otherhand the UFB and CCB constraints quite often acquire greater eliminating power to rule out significant parts of such regions beyond the striking range of the current experiments. Thus, there is an intricate balance between such ‘potential constraints’ and the expanding SUSY APS. For some values of the free parameters, the UFB and CCB conditions are very sharp and disallow most of the parameter space that is otherwise allowed; for some other values, they lose their constraining power.

In a very interesting paper which revived interest in UFB and CCB constraints, Casas *et al* [3] investigated such constraints on SUSY models. Though their formulae are fairly model-independent, they have carried out the numerical analysis for moderate values of $\tan \beta$ (the ratio of the vacuum expectation values (VEV) of the two Higgs fields) only, when one can ignore the effects of b and τ Yukawa couplings in the relevant renormalization group equations (RGE’s). Further they have used the standard minimal supergravity (MSUGRA) assumption of universal soft scalar mass m_0 and universal gaugino mass $m_{1/2}$ at the GUT scale M_G , referred to hereafter as the ‘conventional scenario’, to determine the sparticle spectrum. Their main result was that within the framework of MSUGRA, a certain UFB constraint known as UFB-3 with VEV given in the direction of the slepton field puts the tightest bound on the SUSY parameter space that they considered (see eq. (93) of [3] and the discussions that follows).

The purpose of this work is to extend and complement the work of [3] by analyzing the effectiveness of the UFB constraints for large $\tan \beta$. This we have done in two models: (i) the conventional scenario and (ii) a modified version of MSUGRA within the frame of a SO(10) GUT where the sfermion soft masses m_{16} are universal at the GUT scale, but the Higgs soft masses m_{10} are different from them (this we will call the ‘nonuniversal scenario’). In course of this work we have realized that in contrast to the low $\tan \beta$ scenario, the UFB-3 constraint with squarks (eq. 31 of [3]) may become stronger under certain circumstances, and over a large part of the parameter space the constraint known as UFB-1 (see eq. (8)) serves as the chief restrictor of the APS.

It is well known that there are quite a few motivations for going beyond small and intermediate values of $\tan \beta$ in the context of Grand Unified Theories (GUT). If one assumes the GUT group SO(10) breaking directly to the SM gauge group SU(3)×SU(2)×U(1), and a minimal Higgs field content (only one **10** containing both the light Higgs doublets required in MSSM),

¹ Apart from the fact that they should not be more than a few TeV if we have to have an acceptable solution to the hierarchy problem, there is no hint from the theory about their actual values.

the top, bottom and τ Yukawa couplings must unify to a definite GUT scale value at the scale where $\text{SO}(10)$ breaks [4]. Within the framework of GUTs partial $b - \tau$ Yukawa unification is also an attractive possibility [5, 6]. In an $\text{SO}(10)$ model, even if one assumes more than one **10**-plet of Higgs fields, τ and bottom Yukawa couplings must unify, but the top Yukawa may not unify with them at the GUT scale M_G .

It can be shown that $\tan\beta$ must lie in the range 45-52 for $t - b - \tau$ Yukawa unification (for $m_t = 175$ GeV) and in the range 30-50 for only $b - \tau$ unification. We do not consider the possibility $\tan\beta \leq 2$ since such low values of $\tan\beta$ are now under pressure due to the lower bound on the lightest Higgs boson mass from LEP [7]. This justifies the enthusiasm that has been generated regarding the phenomenology of large $\tan\beta$ scenario [8, 9].

To motivate the nonuniversal scenario under consideration, let us note that from a SUGRA point of view, it is natural to choose the scale at which SUSY breaks in the vicinity of the Planck scale $M_P \approx 2.4 \times 10^{18}$ GeV. At this scale, one may have truly universal soft masses for all scalars; however, the running of the scalar masses between M_P and M_G can lead to a nondegeneracy at M_G [10]. Within the framework of an $\text{SO}(10)$ GUT, the first two sfermion generations will still be degenerate, as they live in the same representation of $\text{SO}(10)$ and have negligible Yukawa couplings. The Higgs fields live in a different representation, and couple to other heavy GUT fields to generate the doublet-triplet splitting; so their masses can change significantly. The third generation sfermions may have a large Yukawa coupling and hence may be nondegenerate from the first two generation of sfermions, though this effect has not been taken into account in our discussion for simplicity. Only the Higgs mass parameter (m_{10}) at M_G is assumed to be different from the common soft sfermion mass (m_{16}) at that scale, and both are treated as free parameters.

In addition to restricting the values of $\tan\beta$, the requirement of Yukawa unification eliminates a significant region of the otherwise large APS of MSSM quite effectively. For example, this unification occurs within a rather limited region of the $m_{16} - m_{1/2}$ plane for certain generic choices of the common trilinear soft breaking parameter A_0 . This dependence arises largely through the radiative corrections to the running bottom quark mass [11] which in turn controls the bottom quark Yukawa coupling λ_b at low energies. The UFB-1 and the UFB-3 conditions further eliminate a significant region from this already restricted APS, which is one of the main results of this paper. Throughout the paper we ignore the possibility that the nonrenormalizable effective operators may stabilise the potential [12].

The APS obtained by requiring Yukawa unification only is quite sensitive on the choice of A_0 . For example, in the conventional scenario with $b - \tau$ unification, the APS increases quite a bit for large negative values of A_0 . It is precisely these values of A_0 which makes the potential more vulnerable to the UFB conditions and many of the additional points allowed by choosing A_0 appropriately are eliminated by the UFB conditions, as will be demonstrated in a later section. Thus, there is a nice complementary behaviour: for large negative A_0 , the Yukawa unification criterion is a weak condition but UFB conditions are very strong, while for small negative values of A_0 the roles are reversed. For positive A_0 , none of these criteria are sufficiently strong.

Following the same procedure, significant regions of the parameter space can be eliminated for models with $t - b - \tau$ Yukawa unification. In particular, we find that $A_0 \leq 0$ is completely ruled out.

The effectiveness of Yukawa unification as a restrictor of the APS also diminishes, as expected, as the accuracy with which we require the unification to hold good is relaxed. There are several reasons why the unification may not be exact. First, there may be threshold corrections [13], both at the SUSY breaking scale (due to nondegeneracy of the sparticles) and at M_G , of which no exact estimates exist. Secondly, we have used two-loop RGE's for gauge couplings as

well as Yukawa couplings and one loop RGEs for the soft breaking parameters, but higher order loop corrections may be important at a few percent level at higher energy scales. Finally the success of the unification program is also dependent on the choice of $\alpha_s(M_Z)$ which is not known as precisely as α_1 or α_2 . To circumvent such drawbacks, one relaxes the Yukawa unification condition to a finite amount (5%, 10% or 20%) which should indirectly take care of these possible caveats. It is interesting to note that quite often the UFB constraints rule out substantial parts of the extended APS.

Some of the “potential” constraints analyzed here were also discussed by Rattazzi and Sarid [4]. However, they considered the RG improved tree-level potentials only and included the possibility of stabilizing the potential through nonrenormalizable effective operators. Moreover the potent UFB-3 constraint was not available at the time of their analysis. Finally a systematic analysis of the APS in the $m_{1/2}$ - m_{16} plane, which is very relevant for physics studies at the Large Hadronic Collider (LHC), was not presented.

When the $SO(10)$ symmetry breaks down to the SM symmetry, there may be a nonzero D-term, which causes the mass splitting between sfermions in $\mathbf{5}$ and $\overline{\mathbf{10}}$ of $SO(10)$ [14]. Recently, a number of authors addressed to the phenomenology of the $SO(10)$ D-terms [15]. In this paper, we take the D-term to be zero for simplicity; with a nonzero D-term, one gets a wider variety of constraints which will be discussed in a subsequent paper [16].

It is well-known that there is a basic conflict between $b \rightarrow s\gamma$ and $t-b-\tau$ Yukawa unification. The latter works best for $\mu < 0$ and large $\tan\beta$, while at the same time this region of the parameter space tends to give unacceptable contributions to the former [17]. However, in view of the uncertainties in the long-distance corrections and the possibility of cancellation between various diagrams, we have not included this constraint in our analysis.

The plan of the paper is as follows. In the next section, we outline the various UFB directions of the supersymmetric potential, and discuss our methodology. The next section deals with the results and in the last section, we summarize and conclude.

2 UFB Directions of the SUSY potential

In this section we briefly review the necessary formulae for the UFB directions following [3] and [18]. We closely follow the former reference in defining the said directions.

The scalar potential of the MSSM is a function of several scalar fields. An $SU(2) \times U(1)$ breaking minimum of this potential must exist for preserving the phenomenological successes of the SM. Moreover, one demands this real minimum $V_{realmin}$ to be deeper than the unwanted UFB and CCB minima. These minima are computed by giving VEV to one or more scalar components at a time; the condition is that at no point in such dangerous directions the potential should be deeper than $V_{realmin}$. The resulting constraints on the field space are of much importance as they can restrict the soft SUSY breaking parameters, and hence the sparticle masses and couplings [2]. Let us see how these dangerous field directions arise.

The tree level scalar potential in the MSSM can be written as the sum of the D-term, the F-term and the soft mass term:

$$V_0 = V_F + V_D + V_{soft} \quad (1)$$

where

$$V_F = \sum_{\alpha} \left| \frac{\partial W}{\partial \phi_{\alpha}} \right|^2,$$

$$\begin{aligned}
V_D &= \frac{1}{2} \sum_a g_a^2 \left(\sum_\alpha \phi_\alpha^\dagger T^a \phi_\alpha \right)^2, \\
V_{soft} &= \sum_\alpha m_{\phi_\alpha}^2 |\phi_\alpha|^2 + \sum_i \{ A_{u_i} \lambda_{u_i} Q_i H_2 u_i + A_{d_i} \lambda_{d_i} Q_i H_1 d_i + A_{e_i} \lambda_{e_i} L_i H_1 e_i + h.c. \} \\
&\quad + (B\mu H_1 H_2 + h.c)
\end{aligned} \tag{2}$$

and the superpotential W is defined as

$$W = \sum_i \{ \lambda_{u_i} Q_i H_2 u_i + \lambda_{d_i} Q_i H_1 d_i + \lambda_{e_i} L_i H_1 e_i \} + \mu H_1 H_2. \tag{3}$$

Here, ϕ_α are the generic scalar fields, T_a and g_a are the gauge group generators and the gauge couplings respectively, and λ 's are the respective Yukawa couplings. A_i , B and m_i are the soft SUSY breaking parameters, and μ is the Higgsino mass term. In eq. (3) Q_i and L_i stand for SU(2) doublet squark and slepton superfields while u, d and e are the corresponding singlet superfields. The generation index i runs from 1 to 3.

The neutral part of the Higgs potential in the MSSM is given by

$$V_{Higgs} = m_1^2 |H_1|^2 + m_2^2 |H_2|^2 - 2 |m_3^2| |H_1| |H_2| + \frac{1}{8} (g'^2 + g_2^2) (|H_2|^2 - |H_1|^2)^2 \tag{4}$$

where $m_1^2 = m_{H_1}^2 + \mu^2$, $m_2^2 = m_{H_2}^2 + \mu^2$, and $m_3^2 = -\mu B$, with m_{H_1} and m_{H_2} being the mass terms of the two doublets. The standard GUT normalization is used for the gauge couplings: $g_3 = g_2 = g_1 = \sqrt{5/3} g'$ at M_G . Minimization of this tree-level potential yields

$$V_{realmin} = - \frac{\{ [(m_1^2 + m_2^2)^2 - 4|m_3^2|^4]^{1/2} - m_1^2 + m_2^2 \}^2}{2(g'^2 + g_2^2)}. \tag{5}$$

At any scale Q , there is a significant radiative correction to this potential. Including the one-loop corrections, the potential becomes

$$V = V_0 + \Delta V_1 \tag{6}$$

where

$$\Delta V_1 = \sum_\alpha \frac{n_\alpha}{64\pi} M_\alpha^4 \left[\ln \frac{M_\alpha^2}{Q^2} - \frac{3}{2} \right], \tag{7}$$

with $n_\alpha = (-1)^{2s_\alpha} (2s_\alpha + 1)$, s_α being the spin of the corresponding field. One ensures the minima of H_1 and H_2 at $|H_1| = v_1$ and $|H_2| = v_2$ with $M_W^2 = \frac{1}{2} g^2 (v_1^2 + v_2^2)$.

As was pointed out, the constraints on the APS arise from directions in the field space along which the potential becomes lower than $V_{realmin}$ (and may become unbounded from below). However, the minimization of the full potential V is rather cumbersome. On the otherhand, just minimizing the tree-level potential at the weak scale neglecting ΔV_1 can lead to quite erroneous conclusions about the minimum point in the field space as was shown by [18]. As a compromise, one evaluates V at a judiciously chosen scale \hat{Q} where the one-loop correction is minimum. As is evident from eq. (7), this scale should be about the typical SUSY mass scale M_S so that the large logarithmic terms tend to vanish.

The dangerous directions are selected in such a way that the positive definite F-terms vanish and the D-terms either cancel each other or their magnitudes can be kept under control. There are several other guidelines as discussed in [3]. Using these conditions one can get the following UFB potentials.

UFB-1: The condition

$$m_1^2 + m_2^2 \geq 2 |m_3^2|, \tag{8}$$

which is known as UFB-1, must be satisfied at any scale $\hat{Q} > M_S$, and particularly at the unification scale $\hat{Q} = M_G$, to have a realistic minimum of the scalar potential. From eq. (8), small $m_{H_1}^2$ (and $m_{H_2}^2$) makes the UFB-1 condition severely restrictive. This may be the case for large $\tan\beta$ and large negative values of A_0 . The variations of $m_{H_1}^2$ and $m_{H_2}^2$ in the conventional scenario with respect to the common trilinear coupling A_0 for $\tan\beta = 30$ and 45, corresponding to $b - \tau$ and $t - b - \tau$ Yukawa unification respectively, are illustrated in fig. 1. From the figure we find that negative values of A_0 drive $m_{H_2}^2$ to large negative values in both the cases. For $m_{H_1}^2$ the effect is prominent for large $\tan\beta$, while for $\tan\beta = 30$, $m_{H_1}^2$ remains positive for most of the range of A_0 that we have studied. The plot of m_H^2 vs A_0 is also given for different values of $m_{1/2}$ and m_{16} for $\tan\beta = 45$ in figures 2 and 3 respectively. From these plots it is clear that for large $m_{1/2}$ and/or m_{16} , and large negative A_0 , $m_{H_1}^2$ and $m_{H_2}^2$ decrease significantly, so that these values of $m_{1/2}$ and m_{16} become vulnerable to UFB-1. This is the reason why in the large $\tan\beta$ case the UFB-1 constraint plays a very significant role in restricting the APS.

UFB-2: The doublet slepton (along the sneutrino direction) and both H_1 and H_2 are given nonzero VEVs. For any value of $|H_2| < M_G$ satisfying

$$|H_2|^2 > \frac{4m_{L_i}^2}{(g'^2 + g_2^2)[1 - \frac{|m_3|^4}{\mu^4}]}, \quad (9)$$

and provided that

$$|m_3^2| < \mu^2 (= m_1^2 - m_{L_i}^2), \quad (10)$$

the UFB-2 potential is given by

$$V_{UFB-2} = [m_2^2 + m_{L_i}^2 - \frac{|m_3|^4}{\mu^2}] |H_2|^2 - \frac{2m_{L_i}^4}{g'^2 + g_2^2} \quad (11)$$

At any momentum scale \hat{Q} , this should be greater than $V_{realmin}$ for a stable configuration:

$$V_{UFB-2}(Q = \hat{Q}) > V_{realmin}(Q = M_S) \quad (12)$$

where $\hat{Q} \sim \text{Max}(g_2 |H_2|, \lambda_{top} |H_2|, M_S)$. However, we find that UFB-2 hardly rules out any further region of the APS which passes the UFB-1 and UFB-3 constraints, so it is of limited interest to us.

UFB-3: The convention is to choose $H_1 = 0$ and to cancel the H_1 F-term (which is a combination of H_2 and d_{L_i}, d_{R_i} or e_{L_i}, e_{R_i}) with suitable VEVs to H_2 and the abovementioned slepton or squark directions. However, it is economical to give VEVs to the doublet fields (along $T_3 = -1/2$ direction) rather than the singlet fields to cancel both SU(2) and U(1) D-terms at the same stroke. Suppose the sleptons are given VEV; then for any values of $|H_2| < M_G$ satisfying

$$|H_2| > \sqrt{\frac{\mu^2}{4\lambda_{e_j}} + \frac{2m_{L_i}^2}{g'^2 + g_2^2}} - \frac{|\mu|}{2\lambda_{e_j}}, \quad (13)$$

the UFB-3 potential is defined as

$$V_{UFB-3} = [m_2^2 - \mu^2 + m_{L_i}^2] |H_2|^2 + \frac{|\mu|}{\lambda_{e_j}} [m_{L_j}^2 + m_{e_j}^2 + m_{L_i}^2] |H_2| - \frac{2m_{L_i}^4}{g'^2 + g_2^2}. \quad (14)$$

If $|H_2|$ does not satisfy (13), the formula changes to

$$V_{UFB-3} = [m_2^2 - \mu^2] |H_2|^2 + \frac{|\mu|}{\lambda_{e_j}} [m_{L_j}^2 + m_{e_j}^2] |H_2| + \frac{1}{8} (g'^2 + g_2^2) \left[|H_2|^2 + \frac{|\mu|}{\lambda_{e_j}} |H_2| \right]^2 \quad (15)$$

with $i \neq j$. Note that we could substitute squarks for sleptons, where $i = j$ is allowed. The constraints on the parameter space arise from the requirement

$$V_{UFB-3}(Q = \hat{Q}) > V_{realmin}(Q = M_S) \quad (16)$$

where \hat{Q} is chosen to be $\hat{Q} \sim \text{Max}(g_2 |e|, g_2 |H_2|, \lambda_{top} |H_2|, g_2 |L_i|, M_S)$ to minimize ΔV_1 . The VEVs are not arbitrary; they satisfy

$$|e| = \sqrt{|H_2| |\mu| / \lambda_{e_j}}, \quad |L_i^2| = \left(|H_2|^2 + |e|^2 \right) - 4 \frac{m_{L_i}^2}{(g'^2 + g_2^2)}. \quad (17)$$

As can be seen from eq. (14), the region of the parameter space where $m_{H_2}^2 = m_2^2 - \mu^2$ is large and negative is very susceptible to be ruled out by the UFB-3 condition. This is because the first term of eq. (14) may become negative in this case. However, the second term in (14), which is positive definite, may become competitive in certain cases (*e.g.*, for $j = 1$, when the Yukawa coupling in the denominator is small), which directions one should avoid when looking for the dangerous minima.

V_{UFB-3} with sleptons was found to be the strongest among all the UFB and CCB constraints in the low $\tan \beta$ case [3]. In order to get the optimum result one has to take the largest λ_{e_j} in the second term of eq. (14), which leads to the choice $e_j = \tilde{\tau}_R$. Now the restriction $i \neq j$ requires $L_i = \tilde{e}_L$ or $\tilde{\mu}_L$ and excludes the choice $\tilde{\tau}_L$. In the low $\tan \beta$ case this restriction, however, is of little consequence since all the left sleptons are degenerate to a very good approximation.

The UFB -3 constraint with squarks may also be imposed by the following replacements in (14):

$$e \rightarrow d, \quad \lambda_{e_j} \rightarrow \lambda_{d_j}, \quad L_j \rightarrow Q_j \quad (18)$$

(see eq. (31) of [3]). Now i may be equal to j and $\hat{Q} \sim \text{Max}(g_2 |d|, g_2 |H_2|, \lambda_{top} |H_2|, g_2 |L_i|, M_S)$.

Now the optimum choice is $d_j = \tilde{b}_R$. However, since the choice $i = j$ is permitted, $L_i = \tilde{\tau}_L$ is not excluded. At high negative A_0 and at high $\tan \beta$, $m_{\tilde{\tau}_L}$ becomes smaller than the corresponding mass parameters of the first two generations. The variation of left-handed slepton mass parameters with A_0 (for $\tan \beta = 45$) is shown in fig. 4. This relatively small $m_{\tilde{\tau}_L}$ at high $\tan \beta$ may make the alternative choice (18) more restrictive than the UFB-3 condition with sleptons. This, in fact, has been supported by our numerical computations.

3 Results

We now briefly review our methodology for implementing the Yukawa unification and computing the spectrum which is based on the computer program ISASUGRA, a part of the ISAJET package. We use the ISAJET version 7.48 [19].

To calculate Yukawa couplings at $\hat{Q} = M_Z$, we start with the pole masses $m_b = 4.9$ GeV, $m_\tau = 1.784$ GeV and $m_t = 175$ GeV. At $\hat{Q} = M_Z$ the SUSY loop corrections to m_b and m_τ is included using the approximate formulae from ref. [11]. For the top quark Yukawa coupling this correction is added at $\hat{Q} = m_t$. Starting with the three gauge couplings and the t, b and τ Yukawa couplings, we evolve them upto the energy scale M_G . Now the boundary conditions are imposed on the soft breaking parameters according to the conventional or the nonuniversal

scenario, while trial values for the μ and B parameters are taken. Then all parameters are evolved down to the weak scale M_Z . The parameters μ and B are then tentatively fixed at $\hat{Q} = \sqrt{m_{t_L}^- m_{t_R}^-}$ by the radiative $SU(2) \times U(1)$ breaking conditions. Using the particle spectrum so obtained, we compute the radiative corrections to the $SU(2) \times U(1)$ breaking condition, and hence obtain the corrected result for μ and B . The whole process is then repeated iteratively until a stable solution within a reasonable tolerance is achieved. While running down from M_G , the SUSY thresholds are properly taken care of. The renormalization group (RG) equations that we use are upto two-loop for both the gauge couplings and the Yukawa couplings.

The demand of the Yukawa coupling unification at M_G puts an extra constraint on $\tan \beta$. We require unification within an accuracy of 5% for Y_b and Y_τ and 10% for Y_t, Y_b and Y_τ . The accuracy for the latter is relaxed since there are more uncertain factors, *e.g.*, the choice of the Higgs sector. We define three variables $r_{b\tau}, r_{tb}$ and $r_{t\tau}$ where generically $r_{xy} = \text{Max}(Y_x/Y_y, Y_y/Y_x)$. To check whether the couplings unify, we select only those points in the parameter space where $\text{Max}(r_{b\tau}, r_{tb}, r_{t\tau}) < 1.10$ (for $t - b - \tau$ unification) and $r_{b\tau} < 1.05$ (for $b - \tau$ unification). The quark Yukawa couplings depend on $\alpha_s(M_Z)$ which comes out from the gauge unification conditions to be 0.118. Then we impose the experimental constraints $m_{\chi^+} > 95$ GeV, $m_h > 85.2$ GeV and $m_{\tau_1} > 73$ GeV, and require the lightest neutralino to be the lightest SUSY particle (LSP). These constraints filter out the APS on which the potential minima conditions UFB-1 and UFB-3 should apply.

Using μ, B , the gauge and the Yukawa couplings at the GUT scale alongwith the boundary conditions there, we generate the mass spectrum at any scale \hat{Q} using the 26 RG equations of the MSSM. In fig. 5, we show the lightest $\tilde{\tau}, \tilde{t}$ and \tilde{b} masses at the weak scale as functions of A_0 for the conventional scenario with $b - \tau$ Yukawa unification at $m_{16} = 1$ TeV, $m_{1/2} = 500$ GeV (this particular point, for the range of A_0 shown, is allowed by all constraints that we have considered). Note that for $A_0 \lesssim -1.8$ TeV, the lightest stop is the next lightest SUSY particle (NLSP), and is perfectly in the accessible range of the LHC.

We demand the electroweak symmetry to be unbroken at M_G . The Higgs potential is minimized at $\hat{Q} = \sqrt{m_{t_L}^- m_{t_R}^-}$. The proper scale for the UFB potential where the one-loop effects are minimized, as discussed after eq. (15), is chosen by an iterative process within 1% accuracy. Usually a few iterations are sufficient. The UFB potential is calculated for different $|H_2|$ values ranging from zero to M_G , using a logarithmic scale. For each value of $|H_2|$ we compare the UFB potential with the scalar potential of MSSM, and whenever $V_{UFB} < V_{realmin}$, that particular region in the parameter space is marked as disallowed.

It should be emphasized that if the model is subject to the constraint of $b - \tau$ Yukawa unification alone, the allowed region of the $m_{1/2} - m_{16}$ parameter space increases as A_0 becomes more negative. The additional regions of the parameter space thus opened up are, however, severely restricted by the stability conditions on the potential. As a result the region allowed by Yukawa unification in conjunction with the stability of the potential is restricted to a rather small region even for large negative values of A_0 . This will be illustrated by the following numerical results.

We begin our discussion for the allowed parameter space in the $m_{1/2} - m_{16}$ plane for $A_0 = -2m_{16}$ (see fig. 6) in the conventional scenario. At each point μ and $\tan \beta$ have been fixed by the radiative electroweak breaking condition and $b - \tau$ Yukawa unification (at an accuracy of 5%) respectively. As expected from the discussions of the last section, the UFB-1 condition severely restricts the APS for relatively large $m_{1/2}$ and m_{16} . For smaller values of these parameters, the UFB-3 condition takes over; it is interesting to note that for relatively small $m_{1/2}$ and m_{16} , relevant for SUSY searches at the LHC, this condition rules out a small but interesting region of the parameter space. As a result for each $m_{1/2}$ there is an upper limit

on m_{16} and vice versa. Thus for $m_{16} = 500$ (700, 900) GeV we find the gluino mass $m_{\tilde{g}}$ to be definitely less than 749 (1189, 1820) GeV respectively. It may be recalled that in the conventional scenario there is already a lower limit of approximately 300 GeV on $m_{\tilde{g}}$ from the direct searches at the Tevatron [20]. On the otherhand, for $m_{1/2} = 200$ (400, 800) GeV both upper and lower bounds on m_{16} emerge, and we get 590 GeV $(1010, 1775) < m_{\tilde{q}} < 1170$ GeV $(1690, 2200)$ where $m_{\tilde{q}}$ is the average squark mass. Once SUSY signals are seen at the LHC this highly predictive model can be tested.

It may be argued that the accuracy to which Yukawa unification holds is worse than 5% due to the uncertainties discussed in the introduction. Relaxing the accuracy to 10% the region of the parameter space allowed by Yukawa unification alone expands. On imposing various stability conditions, we find that the UFB-1 constraints become somewhat weaker. However, the additional points allowed, especially the ones for low m_{16} , are disallowed by the UFB-3 condition which becomes stronger in this case. As a result the upper bounds on $m_{1/2}$ for relatively small values of m_{16} presented in the last paragraph remain more or less unaltered.

For smaller negative values of $A_0 = -m_{16}$ the UFB constraints become less effective as may be seen from fig. 7. However, the APS is already quite restricted due to the requirement of Yukawa unification alone (this is the complementarity that we have talked about in the introduction). Although the bulk of the restricted APS can be probed at the LHC, a significant region remains inaccessible to it.

As we keep on increasing A_0 (in an algebraic sense) the UFB conditions start losing their effectiveness. For $A_0 = 0$ none of these conditions have any further usefulness in constraining the APS; see fig. 8. However, the stranglehold of Yukawa unification on the APS suffices by itself to predict a restrictive mass spectrum. The m_{16} - $m_{1/2}$ plot is bounded from both below and above, and a significant part of this APS can be probed at the LHC.

For $A_0 > 0$ the UFB conditions become ineffective. Yukawa unification alone yields a loosely restricted APS but most of it lies beyond the kinematic reach of the LHC.

We next focus our attention on the nonuniversal scenario $m_{10} \neq m_{16}$. For a given A_0 , the parameter space allowed by $b-\tau$ Yukawa unification expands considerably from the conventional scenario for $m_{10} < m_{16}$. This is illustrated for $A_0 = -2m_{16}$ in fig. 9 which should be compared with fig. 6. In this case Yukawa unification is achieved for relatively low $\tan\beta$, which in turn makes $m_{H_1}^2$ less negative and hence the UFB-1 constraint weaker to some extent. However, many of the new points so allowed are eaten up by the UFB-3 condition. As a result, there is an upper bound on the allowed values of $m_{1/2}$ for the range of m_{16} studied by us ($m_{16} < 3$ TeV). Moreover, the gluino is most likely to be observed at the LHC for this *entire* range. Also the theoretical lower bound on m_{16} gets stronger. However, the UFB conditions become ineffective as the magnitude of A_0 is reduced keeping its sign negative. At $A_0 = 0$ hardly any point is ruled out by these UFB conditions. This trend is similar to what we obtained for the conventional scenario.

On the otherhand, for $m_{10} > m_{16}$ the APS due to Yukawa unification alone is reduced quite a bit. This is illustrated in fig. 10 with $m_{10} = 1.2m_{16}$, which should be compared with figures 6 and 9. For relatively large m_{16} , UFB-1 is a strong constraint as before, while some portion in the low m_{16} region may be ruled out by the UFB-3 condition. We see that the lower bound on m_{16} is significantly weaker than that in the previous case and m_{16} as low as 300 GeV is allowed. The upper bound on $m_{1/2}$ is also weakened considerably. Yet an observable gluino is predicted over most part of the APS.

We now consider the scenario with $t-b-\tau$ Yukawa unification (within an accuracy of 10%) in the conventional scenario. The UFB-1 condition completely rules out the APS allowed by

the unification criterion alone for $A_0 \leq 0$. (UFB-2 and UFB-3 conditions do not play any major role in constraining the APS.) For $A_0 > 0$, the APS (allowed by Yukawa unification) expands gradually; though a portion of it is ruled out by the UFB-1 constraint, a significant amount still remains allowed, and a sizable fraction of it is accessible at the LHC. The UFB-1 condition gets weaker as we go to larger values of A_0 . In fig. 11, we show the allowed region for $A_0 = 0.3m_{16}$ and $m_{1/2} = m_{16}$; in fig. 12, we introduce nonuniversality by setting $m_{10} = 1.2m_{16}$. Note that in the latter case the APS allowed by Yukawa unification alone is somewhat smaller than that in the conventional MSUGRA scenario.

Lastly, if the accuracy of the Yukawa unification is reduced to some extent (say, to 20%) the APS allowed by the unification criterion alone is significantly enhanced. However, the UFB-1 constraint rules out a large amount of this space, and only a small portion survives for negative A_0 .

To summarize, the APS for large negative A_0 is so restricted by the UFB conditions that one should be able, with a bit of luck, to test the Yukawa unification models that we have discussed at the LHC by checking the squark and gluino masses. This restriction weakens if one goes to algebraically larger values of A_0 . The quantitative nature obviously depends on the model chosen.

4 Conclusions

We have analyzed the consequences of both $b-\tau$ and $t-b-\tau$ Yukawa unifications in conjunction with the UFB conditions in the MSUGRA scenario. In the former case, for $A_0 < 0$, these two constraints nicely complement each other in restricting the APS; when one is weak, the other is sufficiently strong (see figures 6 and 7). For $A_0 \approx 0$ the UFB constraints are rather weak. However, the requirement of Yukawa unification at an accuracy less than 5% by itself squeezes the APS sufficiently. As a result, both $m_{1/2}$ and m_{16} are bounded (see fig. 8 for details) from below as well as above. Bulk of this restricted APS is within the striking range of the LHC. For large positive values of A_0 , both the UFB conditions and the Yukawa unification constraint weaken and a large region of the parameter space accessible at the LHC is permitted.

The most restrictive model that we have studied is the one with $A_0 = -2m_{16}$. Here, mainly due to the UFB-3 constraint, one obtains $m_{\tilde{g}} \lesssim 2$ TeV for $m_0 \lesssim 1$ TeV. Such gluinos are obviously within the reach of the LHC. For $A_0 > 0$, the UFB constraints lose their effectiveness and the loosely restricted APS is rather large.

If the accuracy of $b-\tau$ unification is relaxed, the APS tends to increase as expected. However, the upper bound as mentioned above, *viz.*, $m_{\tilde{g}} \lesssim 2$ TeV for $m_0 \lesssim 1$ TeV more or less holds for large negative A_0 , thanks to the UFB-3 condition.

The requirement of Yukawa unification is less effective in the nonuniversal scenario with $m_{10} < m_{16}$. Nevertheless the model on the whole is quite restrictive due to the UFB constraints. This is illustrated in fig. 9 for $m_{10} = 0.6m_{16}$ and $A_0 = -2m_{16}$. Here a gluino observable at the LHC is almost definitely predicted for $m_{16} \lesssim 3$ TeV. On the otherhand, for $m_{10} > m_{16}$, Yukawa unification by itself strongly constrains the APS (see fig. 10) and the UFB constraints play a subdominant role. Again $m_{\tilde{g}}$ is predicted to be observable at the LHC over most of the APS.

The masses of the third generation of sfermions are expected to be considerably lower than that of the first two generations for large values of $\tan\beta$. In fig. 5 we display in the $b-\tau$ unification scheme, alongwith the UFB conditions, the masses of the lighter stop (\tilde{t}_1), sbottom (\tilde{b}_1) and stau ($\tilde{\tau}_1$) mass eigenstates as functions of A_0 . They are indeed found to be considerably lighter than the sparticles belonging to the first two generations; in fact, the lighter stop could very well be the second lightest SUSY particle. Thus in spite of the restrictions imposed by the

UFB conditions and Yukawa unification, light third generation sfermions can be accommodated. In particular, the possibility that the lighter stop is the NLSP is open for large negative A_0 .

The $t - b - \tau$ Yukawa unification models, with a unification accuracy of 10%, are definitely ruled out for $A_0 \leq 0$ in the conventional scenario. For positive values of A_0 , the UFB-1 condition is less severe, and a portion of the parameter space remains allowed, of which a sizable fraction should be accessible at the LHC. If we relax the accuracy for unification, the APS increases, most of which could be ruled out by the UFB-1 condition.

Acknowledgements

AD thanks Prof. E. Reya for hospitalities at the University of Dortmund. He further thanks both E. Reya and M. Glück for many discussions on the dangerous directions of the scalar potential in supersymmetric theories, and A. Stephan for helps in computation. His work was supported by DST, India (Project No. SP/S2/k01/97) and BRNS, India (Project No. 37/4/97 - R & D II/474). AS acknowledges CSIR, India, for a research fellowship.

References

- [1] For reviews see, *e.g.*, H.P. Nilles, Phys. Rep. **110**, 1 (1984); P. Nath, R. Arnowitt and A. Chamseddine, Applied N=1 Supergravity, ICTP series in Theoretical Physics, vol. I, World Scientific (1984); H. Haber and G.L. Kane, Phys. Rep. **117**, 75 (1985).
- [2] L. Alvarez-Gaumé, J. Polchinski and M. Wise, Nucl. Phys. **B221**, 495 (1983); J.M. Frere, D.R.T. Jones and S. Raby, Nucl. Phys. **B222**, 11 (1983); M. Claudson, L.J. Hall and I. Hinchliffe, Nucl. Phys. **B228**, 501 (1983); C. Kounnas *et al*, Nucl. Phys. **B236**, 438 (1984); J.P. Derendinger and C.A. Savoy, Nucl. Phys. **B237**, 307 (1984); M. Drees, M. Glück and K. Grassie, Phys. Lett. **B157**, 164 (1985); J.F. Gunion, H.E. Haber and M. Sher, Nucl. Phys. **B306**, 1 (1988); H. Komatsu, Phys. Lett. **B215**, 323 (1988).
- [3] J.A. Casas, A. Lleyda and C. Munõz, Nucl. Phys. **B471**, 3 (1996).
- [4] B. Ananthanarayan, G. Lazarides and Q. Shafi, Phys. Rev. **D44**, 1613 (1991); L.J. Hall, R. Rattazzi and U. Sarid, Phys. Rev. **D50**, 7048 (1994); R. Rattazzi and U. Sarid, Phys. Rev. **D53**, 1553 (1996).
- [5] M.S. Chanowitz, J. Ellis and M.K. Gaillard, Nucl. Phys. **B128**, 506 (1977); A.J. Buras *et al*, Nucl. Phys. **B135**, 66 (1978); D.V. Nanopoulos and D.A. Ross, Nucl. Phys. **B157**, 273 (1979), Phys. Lett. **B108**, 351 (1982); J. Ellis, D.V. Nanopoulos and S. Rudaz, Nucl. Phys. **B202**, 43 (1982).
- [6] G.F. Giudice and G. Ridolfi, Z. Phys. **C41**, 447 (1988); M. Olechowski and S. Pokorski, Phys. Lett. **B214**, 393 (1988); P.H. Chankowski, Phys. Rev. **D41**, 2877 (1990); M. Drees and M.M. Nojiri, Nucl. Phys. **B369**, 54 (1992); B. Ananthanarayan, G. Lazarides and Q. Shafi, Phys. Lett. **B300**, 245 (1993); H. Arason *et al*, Phys. Rev. Lett. **67**, 2933 (1991); V. Barger, M.S. Berger and P. Ohmann, Phys. Rev. **D47**, 1093 (1993); M. Carena, S. Pokorski and C.E.M. Wagner, Nucl. Phys. **B406**, 59 (1993); M. Carena *et al*, Nucl. Phys. **B426**, 269 (1994); R. Rattazzi and U. Sarid in [4].
- [7] G. Barenboim, K. Huitu and M. Raidal, hep-ph/0005159.
- [8] H. Baer *et al*, Phys. Rev. Lett. **79**, 986 (1997), Phys. Rev. **D58**, 015007 (1998), *ibid* **D58**, 075008 (1998), *ibid* **D59**, 055014 (1999).

- [9] D. Denegri, W. Majerotto and L. Rurua, Phys. Rev. D**60**, 035008 (1999); I. Hinchliffe and F.E. Paige, Phys. Rev. D**61**, 095011 (2000).
- [10] P. Moxhay and K. Yamamoto, Nucl. Phys. B**256**, 130 (1985); B. Gato, Nucl. Phys. B**278**, 189 (1986); N. Polonsky and A. Pomarol, Phys. Rev. D**51**, 6532 (1995).
- [11] D. Pierce *et al*, Nucl. Phys. B**491**, 3 (1997).
- [12] G. Costa *et al*, Nucl. Phys. B**286**, 325 (1987).
- [13] See, *e.g.*, P. Langacker and N. Polonsky, Phys. Rev. D**47**, 4028 (1993).
- [14] M. Drees, Phys. Lett. B**181**, 279 (1986); Y. Kawamura, H. Murayama and M. Yamaguchi, Phys. Rev. D**51**, 1337 (1995).
- [15] H. Murayama *et al*, Phys. Lett. B**371**, 57 (1996); R. Rattazzi and U. Sarid in [4]; A. Datta, A. Datta and M.K. Parida, Phys. Lett. B**431**, 347 (1998); A. Datta *et al*, Phys. Rev. D**61**, 055003 (2000); H. Baer *et al*, Phys. Rev. D**61**, 111701 (2000).
- [16] A. Samanta, A. Datta and A. Kundu, work in progress.
- [17] M. Carena and C. Wagner, preprint no. CERN-TH-7321-94 (1994); F. Borzumati, M. Olechowski and S. Pokorski, Phys. Lett. B**349**, 311 (1995); M. Carena *et al*, Phys. Rev. D**60**, 075010 (1999).
- [18] G. Gamberini, G. Ridolfi and F. Zwirner, Nucl. Phys. B**331**, 331 (1990).
- [19] H. Baer *et al*, hep-ph/0001086.
- [20] B. Abbott *et al* (D0 Collaboration), Phys. Rev. Lett. **83**, 4937 (1999).

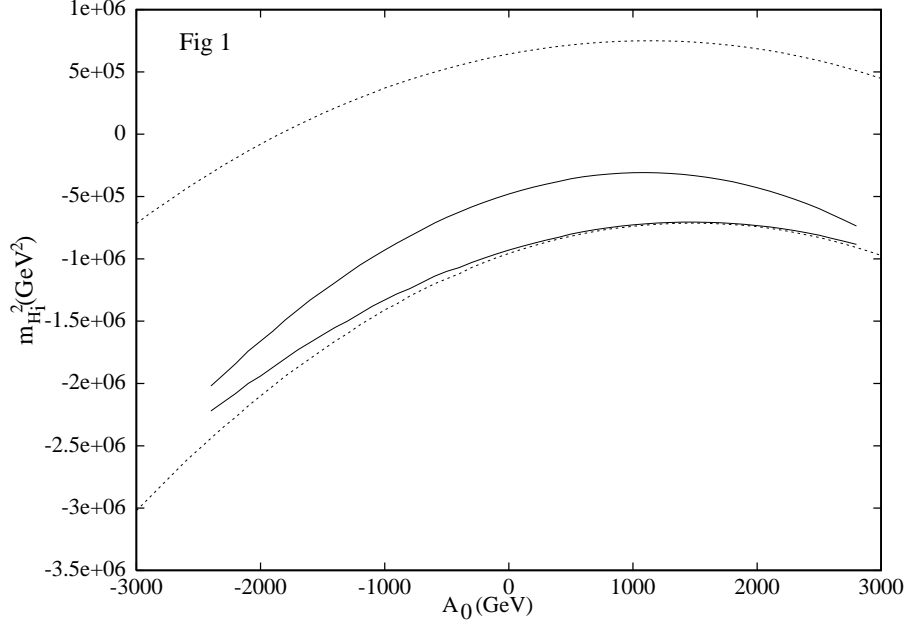


Figure 1: The variation of the Higgs mass parameters $m_{H_1}^2$ and $m_{H_2}^2$ with the trilinear coupling A_0 . The solid (dotted) lines are for $\tan \beta = 45(30)$. The top two lines are for $m_{H_1}^2$ while the lower pair is for $m_{H_2}^2$. We have used $m_{16} = m_{10} = m_{1/2} = 1$ TeV.

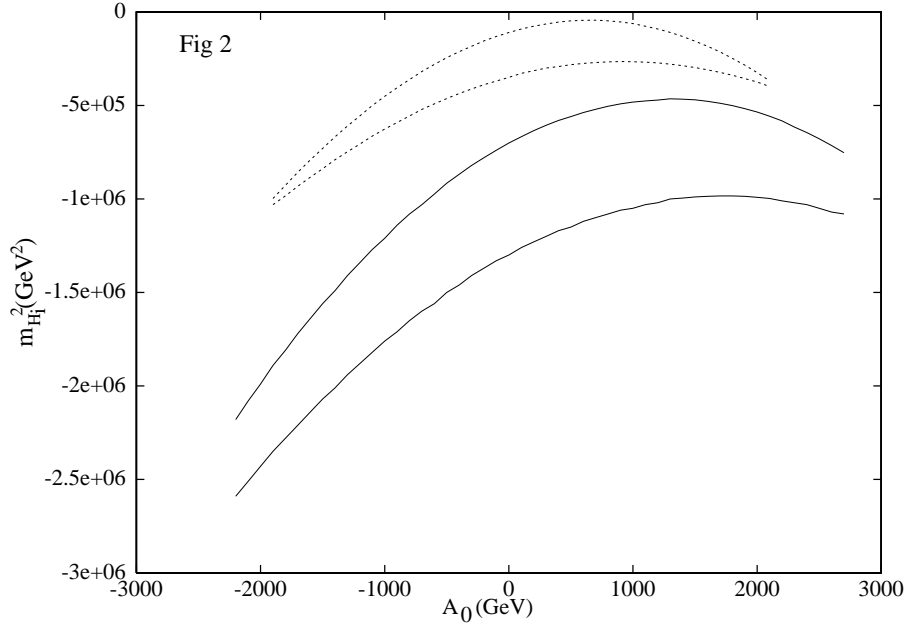


Figure 2: The same variation as shown in figure 1, with two different values of $m_{1/2}$. The dotted (solid) pair is for $m_{1/2} = 600(1200)$ GeV. The upper line in each pair is for $m_{H_1}^2$ and the lower one for $m_{H_2}^2$. $m_{16} = m_{10} = 1$ TeV, $\tan \beta = 45$.

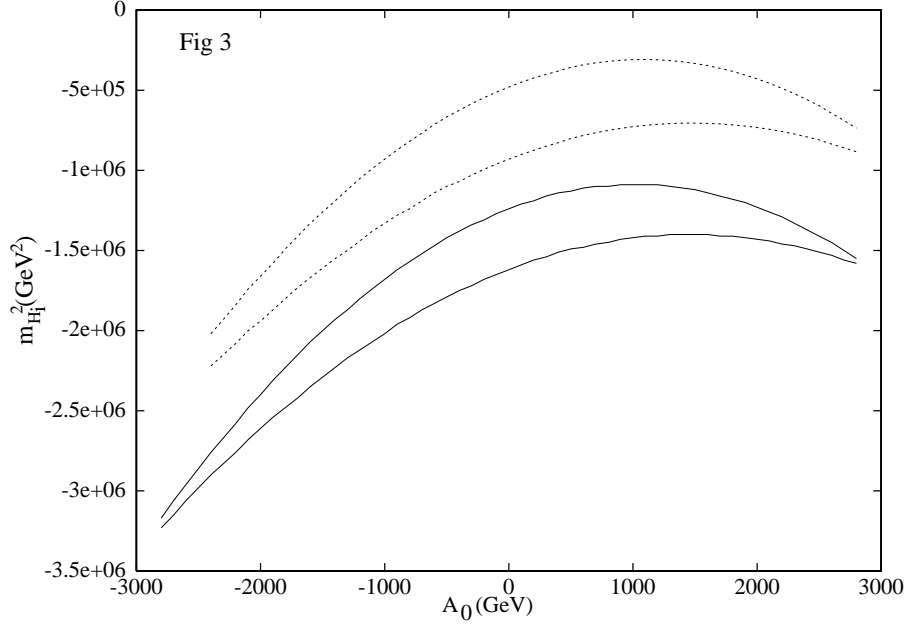


Figure 3: The same variation as shown in Figure 1, with two different values of $m_{16} = m_{10}$. The dotted (solid) pair is for $m_{16} = 1(1.5)$ TeV. The upper line in each pair is for $m_{H_1}^2$ and the lower one for $m_{H_2}^2$. $m_{1/2} = 1$ TeV, $\tan \beta = 45$.

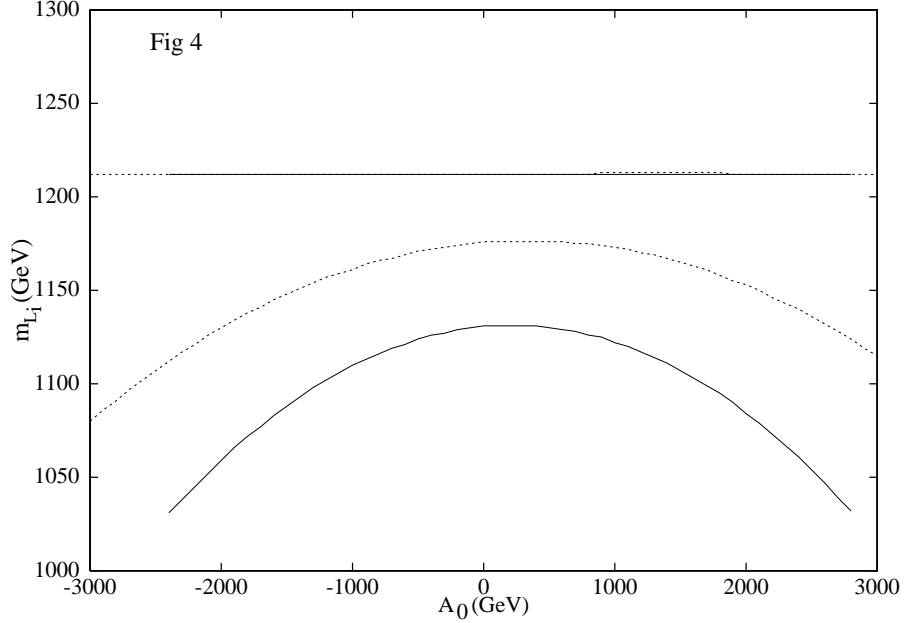


Figure 4: The variation of left-handed slepton mass parameters with A_0 . The dotted (solid) pair is for $\tan \beta = 30(45)$. In each pair, the upper line is for \tilde{e}_L and the lower line for $\tilde{\tau}_L$. Note that the selectron mass is insensitive to the value of $\tan \beta$ and A_0 .

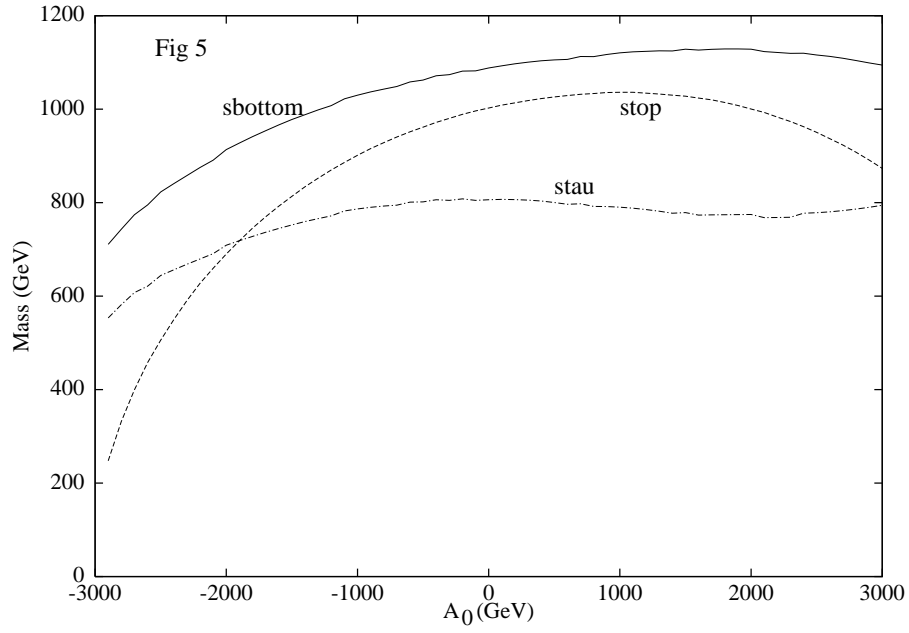


Figure 5: The variation of masses of the lightest $\tilde{\tau}$, \tilde{t} and \tilde{b} with A_0 . We set $m_{16} = m_{10} = 1$ TeV and $m_{1/2} = 500$ GeV. The Yukawa unification condition fixes $\tan\beta$. Note that \tilde{t}_1 can be the second lightest sparticle for $A_0 \lesssim -1.8$ TeV.

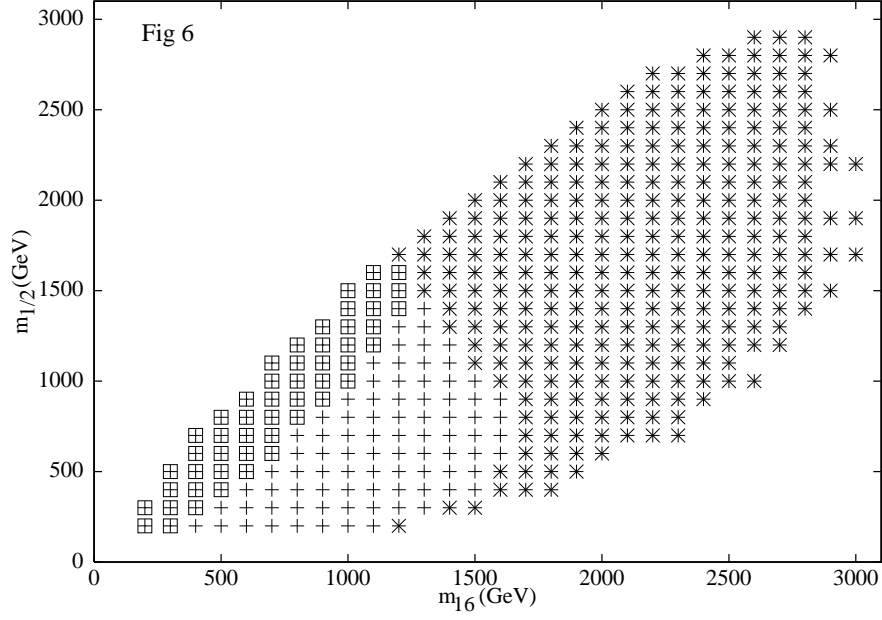


Figure 6: *The allowed parameter space in the conventional scenario with $b - \tau$ unification. All the points are allowed by the Yukawa unification criterion; the asterisks are ruled out by UFB-1 and the boxes by UFB-3. We set $A_0 = -2m_{16}$.*

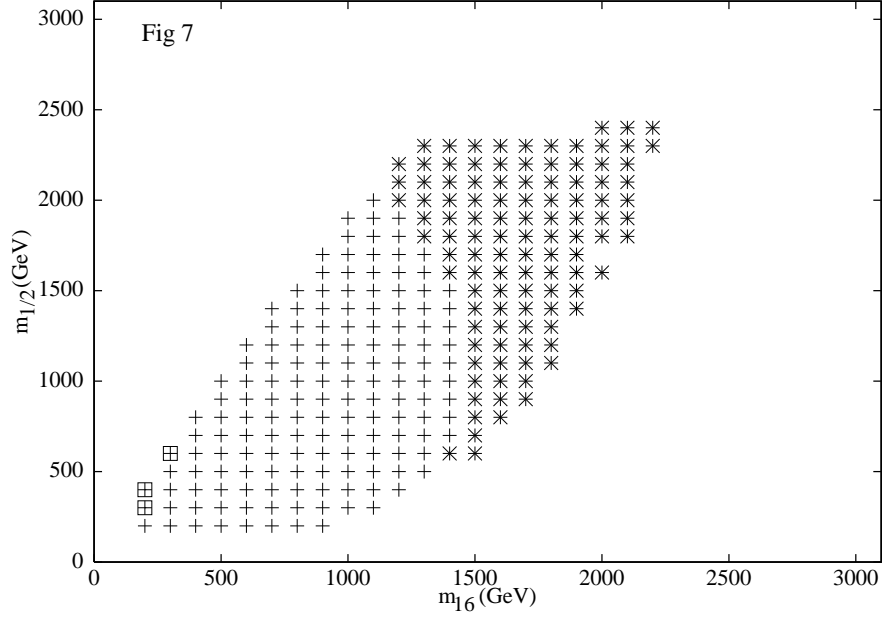


Figure 7: *The same as Fig. 6, with $A_0 = -m_{16}$.*

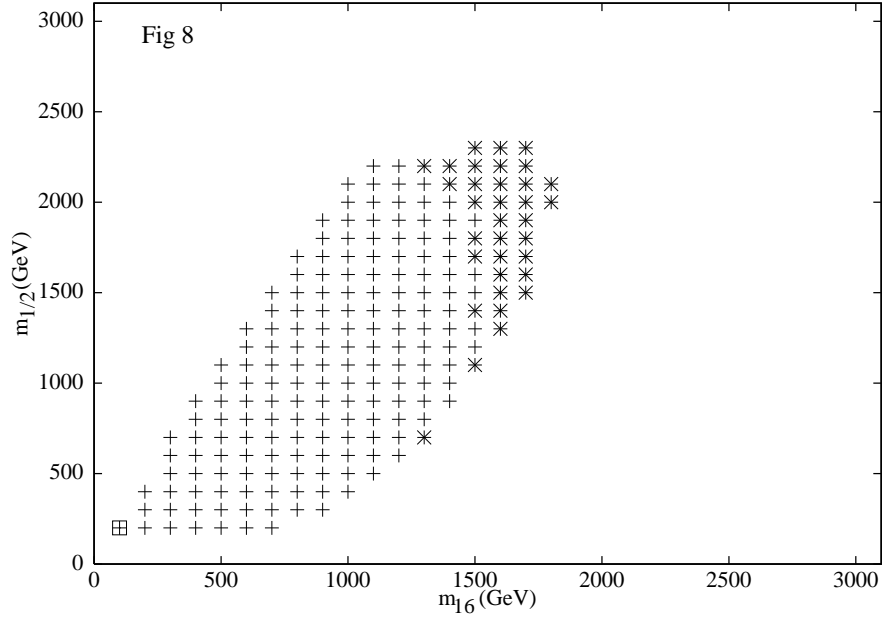


Figure 8: *The same as Fig. 6, with $A_0 = 0$.*

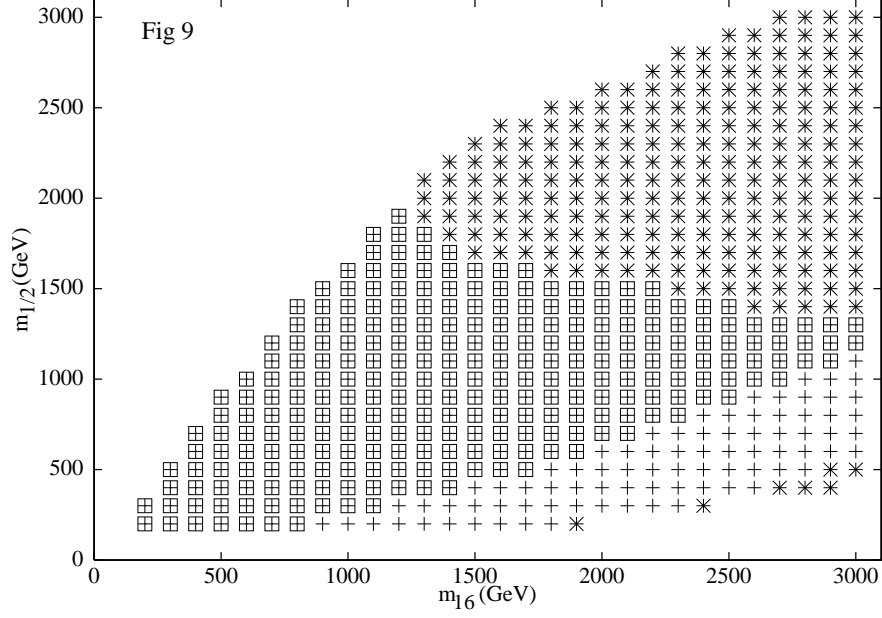


Figure 9: *The allowed parameter space in the nonuniversal scenario with $b - \tau$ unification. All the points are allowed by the Yukawa unification criterion; the asterisks are ruled out by UFB-1 and the boxes by UFB-3. We set $A_0 = -2m_{16}$ and $m_{10} = 0.6m_{16}$.*

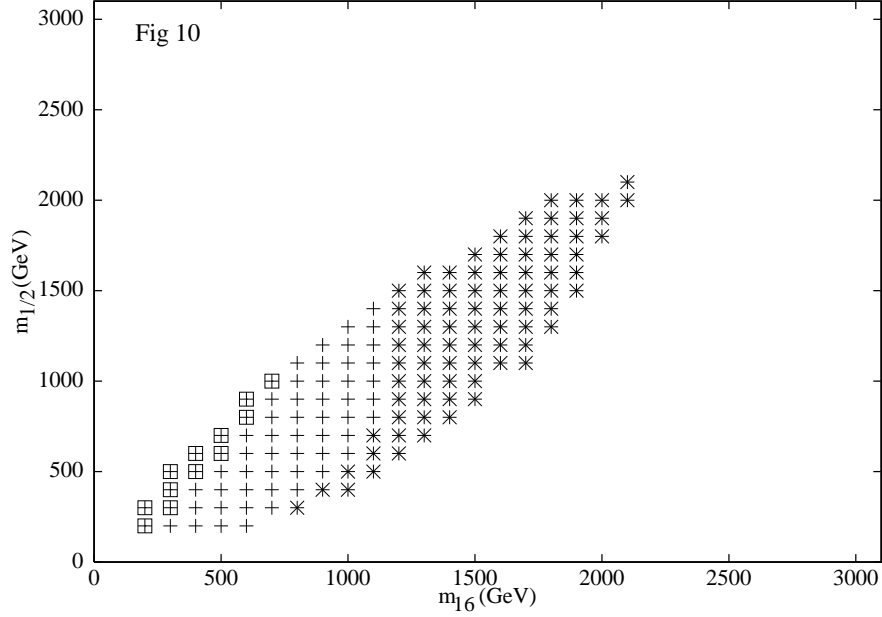


Figure 10: *The same as Fig. 9, with $m_{10} = 1.2m_{16}$.*

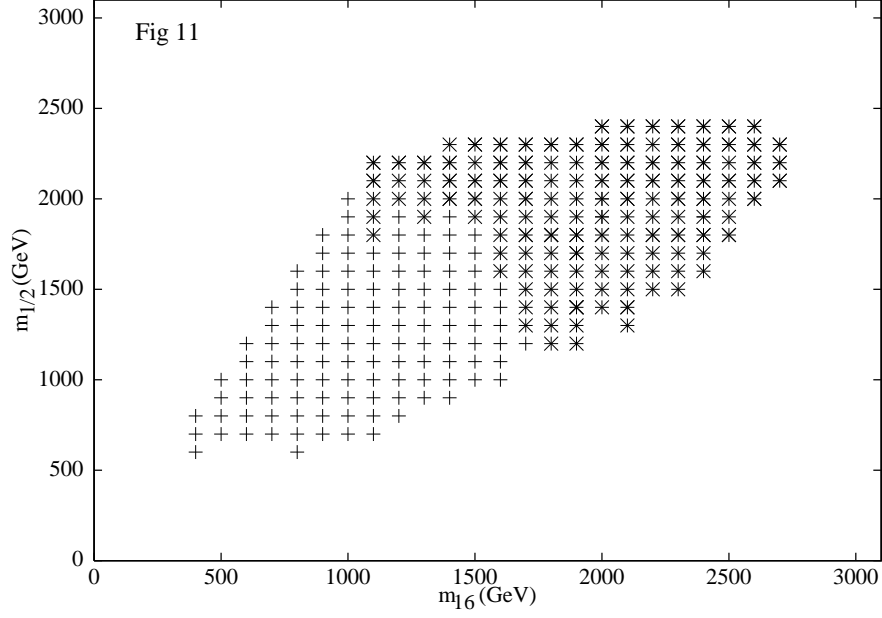


Figure 11: *The allowed parameter space with $t - b - \tau$ unification. Yukawa unification to 10% allows all points, while the asterisks are ruled out by UFB-1. We set $m_{10} = m_{16}$ and $A_0 = 0.3m_{16}$.*

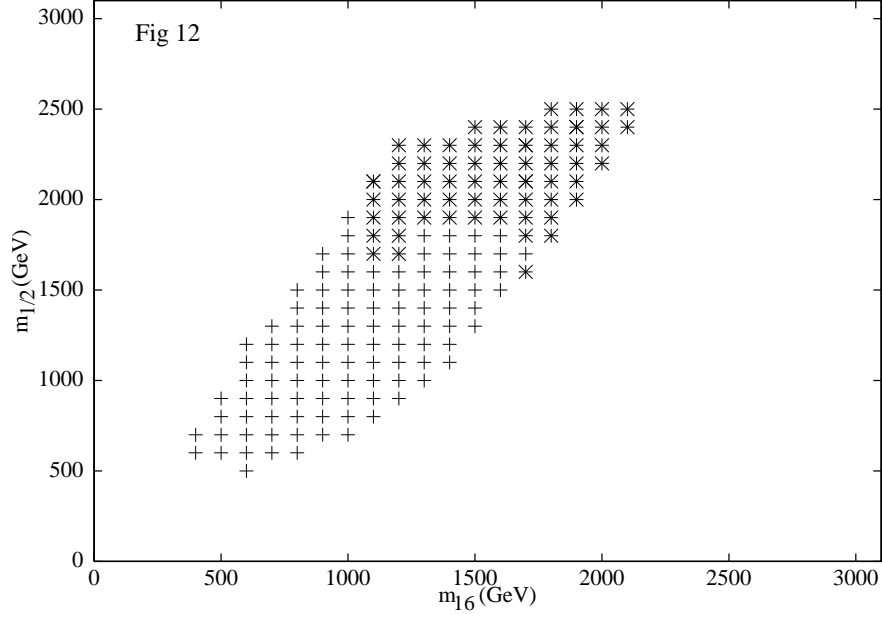


Figure 12: *The same as Fig. 11, with $m_{10} = 1.2m_{16}$.*